[*Geophysical Research Letters*]

Supporting Information for

[**Significant Underestimation in the Optically-based Estimation of the Aerosol First Indirect Effect Induced by the Aerosol Swelling Effect**]

[Jianjun Liu[1,2] and Zhanqing Li[1,3*]]

[[1]Earth System Science Interdisciplinary Center and Department of Atmospheric and Oceanic Science, University of Maryland, College Park, MD, USA.

[2]Laboratory of Environmental Model and Data Optima, Laurel, MD, USA

[3]State Laboratory of Earth Surface Process and Resource Ecology, College of Global Change and Earth System Science, Beijing Normal University, Beijing, China.]

Contents of this file

Text Figure S1, Figure S1, and Figure S2

Text Figure S1

There is good agreement between the two retrievals at both wavelengths and at all sites although the NFOV-measured radiances tend to be underestimated. Zenith radiances at 673 and 870 nm are underestimated by about 20% and 10%, respectively, at the SGP site. At the GRW, PGH, and SX sites, zenith radiances at 673 nm are underestimated by about 10%, 14%, and 11%, respectively. Zenith radiances at 870 nm at these three sites agree well with their corresponding AERONET retrievals. From regression analyses, two-channel NFOV zenith radiances, $F_{673,obs}$ and $F_{870,obs}$, at the SGP site were adjusted using the following formulas:

$$F_{673,adj} = 1.2242 * F_{673,obs} + 0.0003,$$

$$F_{870,adj} = 1.0932 * F_{870,obs} - 0.0001.$$

For the other sites, only measurements at 673 nm were corrected because the measurements at 870 nm agreed well. This correction at each site was done as follows:

$$\text{GRW site: } F_{673,adj} = 1.0984 * F_{673,obs} - 0.0009,$$

$$\text{PGH site: } F_{673,adj} = 1.1357 * F_{673,obs} - 0.0001,$$

$$\text{SX site: } F_{673,adj} = 1.1066 * F_{673,obs} - 0.0007.$$
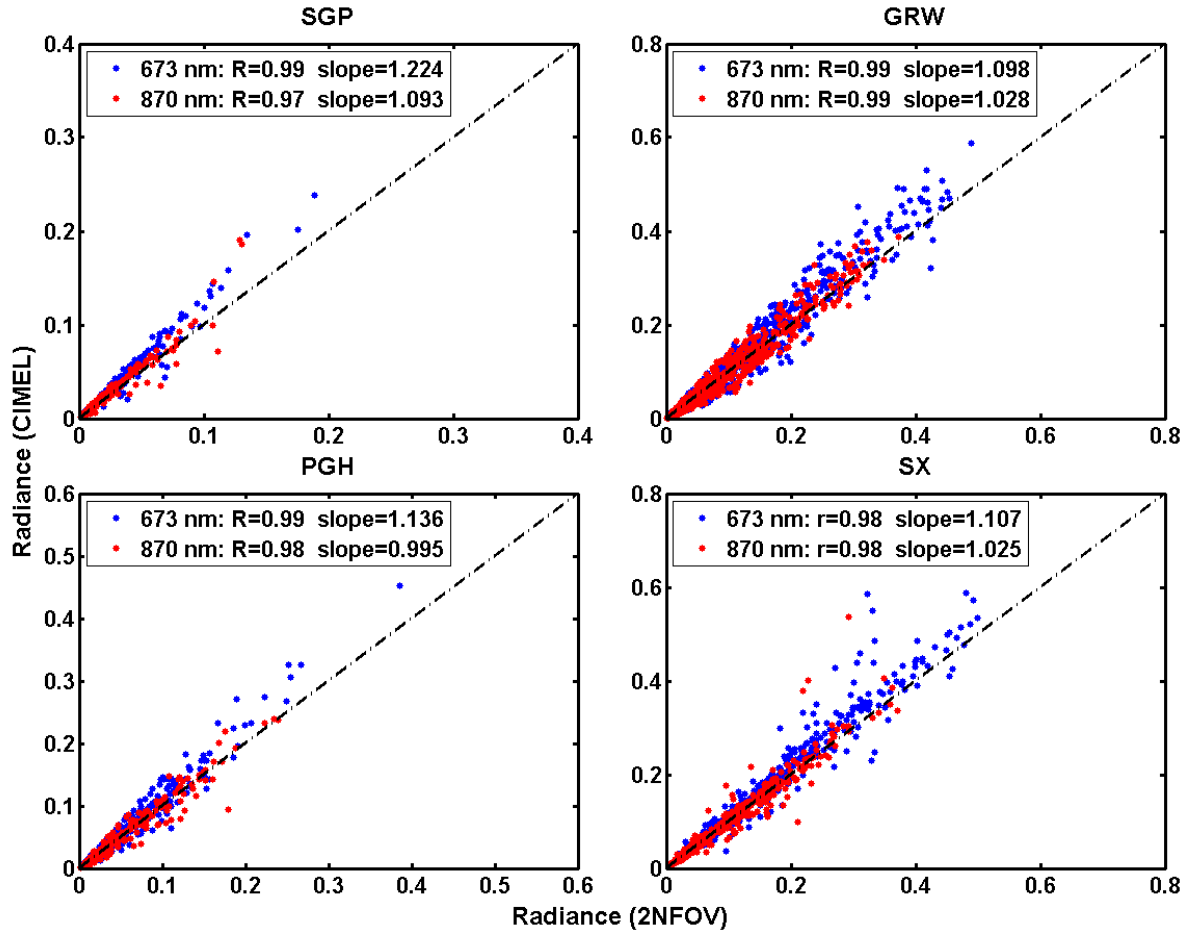
Figure S1. CIMEL Sun photometer-measured radiances at 673 nm (blue dots) and 870 nm (red dots) as a function of corresponding two-channel NFOV measurements at the SGP, GRW, PGH, and SX sites. Slopes of the best-fit lines (not shown) through each group of data are given. Units are W m^{-2} sr^{-1} μm^{-1}. The dash-dot line is the 1:1 line.
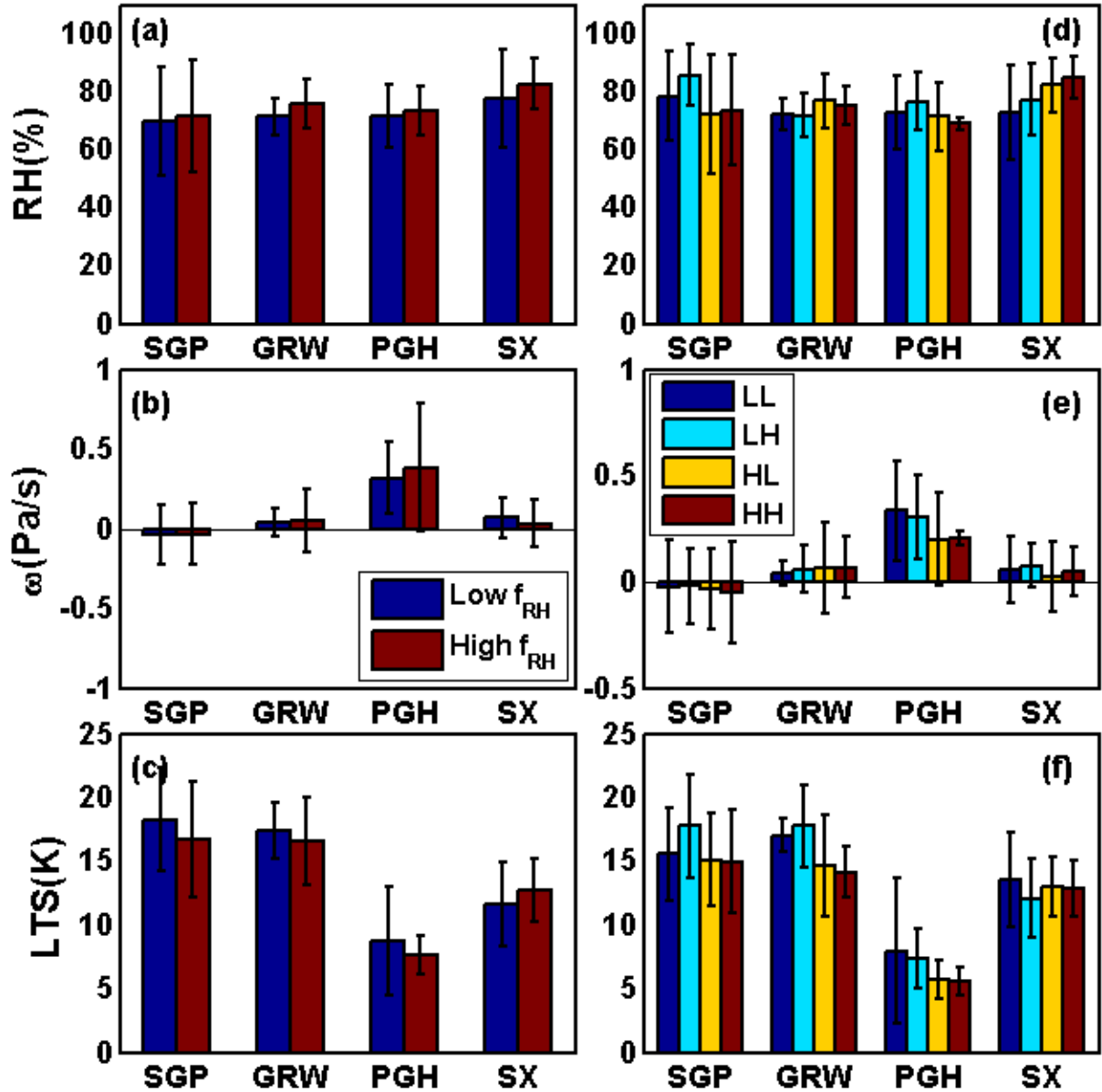
Figure S2. Mean values and standard deviations of (a) relative humidity (RH, %), (b) vertical velocity (ω, Pa s^{-1}), and (c) lower tropospheric stability (LTS, K) for low (blue bars) and high (red bars) f_{RH} cases at the SGP, GRW, PGH, and SX sites. (d) Relative humidity (RH, %), (e) vertical velocity (ω, Pa/s), and (c) lower tropospheric stability (LTS, K) under low f_{RH} and low aerosol loading conditions (LL, blue bars), low f_{RH} and high aerosol loading conditions (LH, cyan bars), high f_{RH} and low aerosol loading conditions (HL, yellow bars), and high f_{RH} and high aerosol loading conditions (HH, red bars) at the SGP, GRW, PGH, and SX sites.

Supporting Information for

[**Significant Underestimation in the Optically-based Estimation of the Aerosol First Indirect Effect Induced by the Aerosol Swelling Effect**]

[Jianjun Liu[1,2] and Zhanqing Li[1,3*]]

[[1]Earth System Science Interdisciplinary Center and Department of Atmospheric and Oceanic Science, University of Maryland, College Park, MD, USA.

[2]Laboratory of Environmental Model and Data Optima, Laurel, MD, USA

[3]State Laboratory of Earth Surface Process and Resource Ecology, College of Global Change and Earth System Science, Beijing Normal University, Beijing, China.]

Contents of this file

Table S1, Table S2, and Table S3

Table S1. Description of ACRF[1] fixed and mobile sites.

Site[2]	Location	Altitude	Time Range	Environment	Measurements[3]
SGP	36.6°N, 97.5°W	320 m	Sep. 2004-Feb. 2005	Agriculture	✧ σ_s and f_{RH} from AOS
GRW	39.1°N, 28.0°W	15 m	Sep. 2009-Aug. 2010	Marine	✧ Surface RH, ω at 700 hPa and LTS
PGH	29.4°N, 79.5°E	1900 m	Jun. 2011-Dec. 2011	Industrial emission/biomass burning	✧ LWP from MWR/MWRP
SX	32.6°N, 116.8°E	20 m	Jun. 2008-Dec. 2008	Industrial emission	✧ COD from 2NFOV

[1] ACRF: Atmospheric Radiation Measurement (ARM) Climate Research Facility

[2] SGP: Southern Great Plains, USA; GRW: Graciosa Island, Azores; PGH: Ganges Valley region, India; SX: ShouXian, Anhui, China

[3] AOS: Aerosol Observing System; σ_s: aerosol scattering coefficient; f_{RH}: aerosol hygroscopic growth factor; RH: relative humidity; ω: vertical velocity at 700 hPa; LTS: lower tropospheric stability; LWP: liquid water path; MWR/MWRP: Microwave Radiometer/ Microwave Radiometer Profiler; 2NFOV: two-channel Narrow Field of View Zenith Radiometer

Table S2. Statistics summarizing cloud microphysical and aerosol hygroscopic/optical properties at each site during their respective study periods.

Site	LWP (g m^{-2})		COD		DER (μm)		$f_{RH\ (85\%/40\%)}$		σ_s (Mm^{-1})	
	Mean	**Median**	**Mean**	**Median**	**Mean**	**Median**	**Mean**	**Median**	**Mean**	**Median**
SGP	151±89	131	35.9±18.2	33.8	7.0±3.3	6.3	1.87±0.41	1.76	45.3±33.9	36.0
GRW	152±104	119	31.8±17.6	26.6	7.9±4.3	7.0	2.22±0.53	2.21	33.8±23.3	27.7
PGH	192±141	142	38.4±21.5	34.0	8.3±4.9	7.1	1.39±0.18	1.40	165.0±119.6	136.2
SX	171±119	127	37.3±24.9	28.8	8.1±4.3	7.1	1.66±0.19	1.67	451±477	328

[*]LWP: liquid water path; COD: cloud optical depth; DER: cloud droplet effective radius; $f_{RH\ (85\%/40\%)}$: hygroscopic growth factor at RH = 85% and reference RH = 40%; σ_s at 450 nm under dry RH conditions for particles with radii less than 10 μm.

Table S3. Means and standard deviations of σ, COD, and DER at each site for cases shown in Figure 1.

	SGP		GRW		PGH		SX	
	$f_{RH} \leq 1.8$	$f_{RH} > 1.8$	$f_{RH} \leq 2.0$	$f_{RH} > 2.0$	$f_{RH} \leq 1.4$	$f_{RH} > 1.4$	$f_{RH} \leq 1.6$	$f_{RH} > 1.6$
σ (Mm⁻¹)	86.7±52.1	50.9±31.9	22.4±20.1	43.3±19.1	256.4±129.2	191.5±123.9	273.3±126.5	319.1±122.4
COD	26.3±5.3	20.5±6.7	22.0±9.0	26.3±9.3	26.5±12.3	25.4±12.9	18.2±10.3	20.5±10.0
DER (μm)	6.0±3.2	6.5±3.5	6.2±2.3	5.0±2.0	6.5±4.3	6.7±3.5	8.6±4.1	7.2±3.5